Am. J. Hum. Genet. 65:1359–1367, 1999

Methylation Imprinting of *H19* and *SNRPN* Genes in Human Benign Ovarian Teratomas

K. Miura,[1,2] M. Obama,[2] K. Yun,[3] H. Masuzaki,[2] Y. Ikeda,[2] S. Yoshimura,[2] T. Akashi,[1] N. Niikawa,[1] T. Ishimaru,[2] and Y. Jinno[1,*]

Departments of [1]Human Genetics and [2]Obstetrics and Gynecology, Nagasaki University School of Medicine, Nagasaki; and [3]Department of Pathology, University of Otago Medical School, Dunedin, New Zealand

Summary

In humans, studies of female germ cells are very limited by ethics. The current study investigated the usefulness of benign ovarian teratomas as a substitute for ova in analyses of imprinted genes. Twenty-five human benign ovarian teratomas were typed with 45 microsatellite DNA markers and classified according to their genotypic features. Two oppositely imprinted genes, *H19* and *SNRPN*, were then chosen for analysis of their methylation states in these tumors. These analyses revealed that benign ovarian teratomas consist of a mixture of genetically and epigenetically heterogeneous cell populations. In contrast to previous reports, we could document only one case rising from germ cells by meiosis-II nondisjunction. *H19* and *SNRPN* were methylated in individual teratomas to various degrees, ranging from normal somatic cell to expected ovum levels. The allele with residual methylation of *H19* was consistent with that methylated in the patient's blood DNA, thus being of paternal origin. Degrees of *H19* hypomethylation and *SNRPN* hypermethylation increased as the cellular origin of the tumors advanced in oogenesis and were closely correlated in individual teratomas. These results could be best explained by the assumption that the primary imprinting is a progressively organized process and suggest that the establishment of primary imprints on different genes might be mechanistically linked, even when those genes are oppositely imprinted.

Received April 2, 1999; accepted for publication August 25, 1999; electronically published October 5, 1999.

Address for correspondence and reprints: Dr. Y. Jinno, Department of Molecular Biology, Ryukyu University School of Medicine, Nishihara, Okinawa 903-0215, Japan. E-mail: sirius@med.u-ryukyu.ac.jp

* Present affiliation: Department of Molecular Biology, Ryukyu University School of Medicine, Nishihara, Okinawa, Japan.

0002-9297/1999/6505-0018$02.00

Introduction

Parent-of-origin–dependent functional differences between maternally and paternally derived chromosomes are referred to as "genomic" or "gametic" imprinting. An outstanding feature of genomic imprinting is its stable and reversible heritability. Although the molecular mechanism of the imprinting is not yet fully unraveled, the maternal and paternal alleles of a gene must be marked in the gamete for the appropriate expression pattern to be assumed and maintained in the embryo. An excellent candidate for the mark is methylation of the cytosine residue in CpG dinucleotides (Razin and Cedar 1994). The most convincing evidence for a role of methylation in imprinting has been obtained in the analysis of methylation and expression of several imprinted genes in methyltransferase-deficient mice (Li et al. 1993).

Although it is widely accepted that methylation is crucially involved in marking alleles and controlling allele-specific expression of imprinted genes, pivotal questions remain with respect to how the imprinting marks are established and erased during gametogenesis. Methylation imprints escape a wave of genomewide demethylation and are protected from a wave of global de novo methylation before and after gastrulation, respectively (Stöger et al. 1993; Tremblay et al. 1995). Phenotypic differences between parthenogenetic (benign ovarian teratomas [MIM 166950]) and androgenetic (complete hydatidiform moles [MIM 231090]) growths are attributable in part to this effect. Analysis of such growths may provide insights into the methylation imprints of the germ cells from which they were generated.

Benign ovarian teratomas (mature cystic teratomas) are composed of fully differentiated mature tissues derived from all three germ layers. They contain a cyst filled with sebaceous material, desquamated squamous cells, and hair and are thought to arise from defects in the meiotic process. An early cytogenetic study indicated that ovarian teratomas were parthenogenetic tumors that arose from a single germ cell after the first meiotic division and failure of meiosis II (Linder et al. 1975).

Later studies using chromosomal heteromorphisms and genetic markers (RFLPs and VNTRs) suggested a diversity of mechanisms in their origin (Dahl et al. 1990; Deka et al. 1990; Surti et al. 1990), and it is now thought that benign ovarian teratomas can originate from each stage of female gametogenesis. The exact nature of the meiotic error that occurred during the formation of a particular teratoma can be inferred by typing with polymorphic DNA markers (fig. 1). Teratomas originating due to a meiosis I error can be expected to be heterozygous for almost all pericentromeric markers, with homozygosity for distal markers being an indicator for crossover events. In contrast, a meiosis II error would produce teratomas in which all markers near the centromere are homozygous, with crossover events reflected by heterozygosity for distal markers. In the present study we used genotyping and methylation analyses of benign ovarian teratomas to investigate whether methylation imprinting of individual genes is an independent and separated process or shares a common process for different genes.

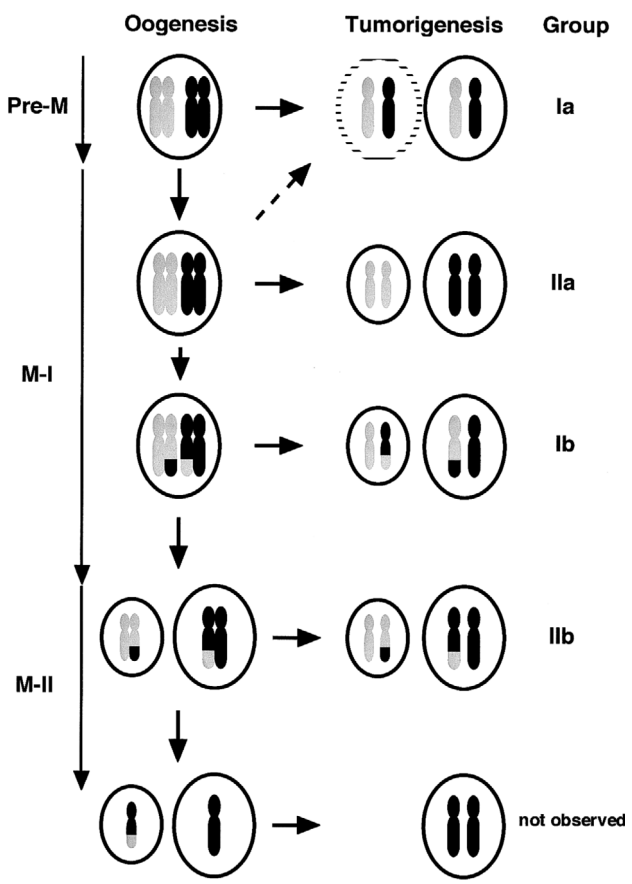

Figure 1 Cellular origin of the teratomas as inferred from the genotype analysis. The smaller circle indicates the minor cell population in the single tumors. "Pre-M" denotes the premeiotic phase, "M-I" denotes the meiosis I phase, and "M-II" denotes the meiosis II phase.

Patients and Methods

Patients

Samples were obtained from 25 patients with mature cystic teratomas who were operated on at the Department of Obstetrics and Gynecology, Nagasaki University Hospital. Tumor samples were collected by one individual, to ensure uniform selection, from July 1996 to April 1998. Informed consent was obtained from patients undergoing surgery. The diagnosis of mature cystic teratoma was confirmed in each case by pathology reports. The teratoma samples were taken from the innermost cell wall or from the growth nidus of the cyst, with care being taken not to include any material from the ovarian capsule, and were washed in sufficient cold saline to exclude contamination by the patient's blood. For each patient, somatic DNA was isolated from a peripheral blood sample. DNA was extracted as described elsewhere (Jinno et al. 1994).

Tissue Culture

Two cases of teratoma (numbers 24 and 25) were subjected to primary cultures. In brief, tissue samples were minced and dissociated with a 0.8% collagenase/0.02% DNase I solution. The cells were grown in Amino Max C-100 (GIBCO-BRL) at 37°C in a humidified atmosphere with 5% CO_2. Fresh medium was added every 4–5 d. Once growth was well established, cells were subcultured and harvested. DNA was extracted from cells during the third passage.

Genotyping

A total of 45 polymorphic microsatellite markers (41 CA-repeat and 4 tetranucleotide-repeat markers) were selected from the Généthon databases (Dib et al. 1996) and from the Cooperative Human Linkage Center markers (Murray et al. 1994). The selected markers consisted of 25 pericentromeric markers on 16 chromosomes and 20 nonpericentromeric markers on 3 chromosomes (see the Appendix). By using the DNA sequencer–assisted method with fluorescent microsatellite marker DNAs, we determined the genotypes of each host-teratoma pair (Mansfield et al. 1994). Genomic DNA samples were typed for CA-repeat and tetranucleotide-repeat markers

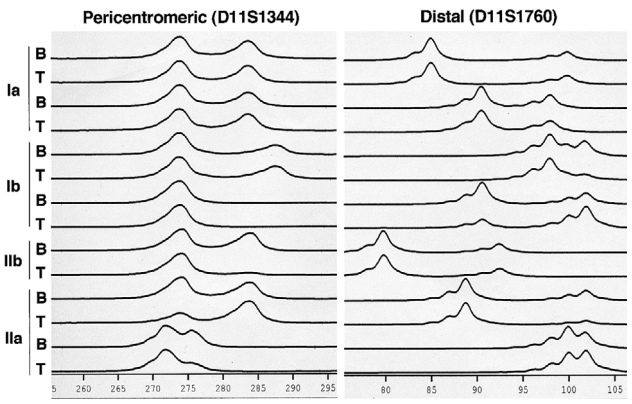

Figure 2 Examples of electrophoretic patterns in microsatellite-repeat markers. Two typical cases in each group except group IIb are demonstrated. B = host-blood DNA; T = tumor-tissue DNA.

by PCR amplification in a 12.5-μl reaction mixture containing 50 ng of genomic DNA, 1 μM each of Cy5-labeled sense primer and unlabeled antisense primer (0.2 mM in each dNTP), 1.25 μl 10 × PCR buffer, and 0.25 U Ampli*Taq* Gold (PE Biosystems). PCR was performed in a GeneAmp PCR System 9600 (PE Biosystems), under the following conditions: 1 cycle at 94°C for 10 min; 40 cycles at 94°C for 30 s, 55°C for 30 s, and 72°C for 30 s; and a final elongation cycle at 72°C for 10 min. A mixture of 4 μl of eightfold-diluted PCR product, 3 μl of loading dye (5 μg dextran blue 2000/μl deionized formamide), and 1.5 μl each of the suitable sized markers (Cy5 Sizer; Pharmacia Biotech) was made. This mixture was denatured at 94°C for 5 min and loaded onto Ready Mix Gel (Pharmacia Biotech) containing 6% acrylamide/bisacrylamide monomers, 100 mM Tris-borate (PH 8.3), and 1 mM EDTA. The DNA was then electrophoresed in a running buffer containing 50 mM Tris-borate and 0.5 mM EDTA, with use of an Automated Laser Fluorescent DNA sequencer (Pharmacia Biotech) at 55°C and 15 W/gel. The resulting data were analyzed with Fragment Manager Version 1.2 software (Pharmacia Biotech), to determine genotypes for marker loci in each subset of host-teratoma pairs. By comparing genotypes of the tumors with those of their hosts, we were able to group them and to assign the stage in oogenesis from which each tumor was likely to have originated.

Methylation Analysis

Southern blot analysis of *H19* methylation was carried out as described elsewhere (Jinno et al. 1996). The probes (*H19* probe 1 and *WT1*/*WIT1* internal control probe) were also the same as those used in the other study. In brief, 5 μg of genomic DNA were digested with *Pst*I and *Pvu*II, then subjected to *Hpa*II digestion (10 U/μg DNA), fractionated onto a 1.6% agarose gel, and transferred to nylon membranes. Signal intensities of the 469-bp *Hpa*II-resistant band and the internal control band were measured on a BAS1000 imaging analyzer (Fujix).

In addition, the methylation state of *SNRPN* was examined at two of the three *Not*I sites present in the exon α-flanking region. Unlike the *H19*-methylation analysis, an internal control was not applied because relative methylation was expressed as ratios of the uncleaved band to a sum of the cleaved and uncleaved bands. Genomic DNA was digested with *Pst*I and *Not*I (15 U/μg DNA) and separated onto a 1.6% agarose gel. A DNA probe was made by use of nested primers on the basis of the GenBank database (accession number U41384). After hybridization, filters were washed to a final stringency of 0.1 × SSC/0.1% SDS at 60°C. PCR conditions (GeneAmp PCR System 9600, PE Biosystems) and primer sequences were as follows: first PCR, 30 cycles with initial denaturation for 4 min at 94°C, subsequent denaturations for 30 s at 94°C, annealing for 30 s at

Table 1

Summary of DNA Typing of 25 Benign Ovarian Teratomas and their Classification

Case	Chromosome Status		No. of Recombinations[a]	Group[b]
	Heterozygous	Homozygous		
1	0	12	0	IIa
2	13	0	0	Ia
3	0	11	0	IIa
4	13	0	0	Ia
5	10	1	6 (3,2,1)	Ib
6	14	0	0	Ia
7	9	1	3 (1,2,0)	Ib
8	8	4	2 (0,2,0)	ND
9	12	0	0	Ia
10	0	9	0	IIa
11	2	9	7 (3,2,2)	IIb
12	12	1	8 (5,1,2)	Ib
13	11	1	3 (2,0,1)	Ib
14	11	0	5 (1,2,2)	Ib
15	12	0	0	Ia
16	11	0	0	Ia
17	0	13	0	IIa
18	11	0	4 (2,1,1)	Ib
19	14	0	0	Ia
20	10	3	2 (0,0,2)	ND
21	8	5	3 (3,0,0)	ND
22	0	14	0	IIa
23	0	12	0	IIa
24	12	0	3 (0,1,2)	Ib
25	14	0	6 (3,3,0)	Ib

[a] Numbers in parentheses are numbers of recombinations on chromosomes 6, 11, and 15, respectively.

[b] ND = not determined.

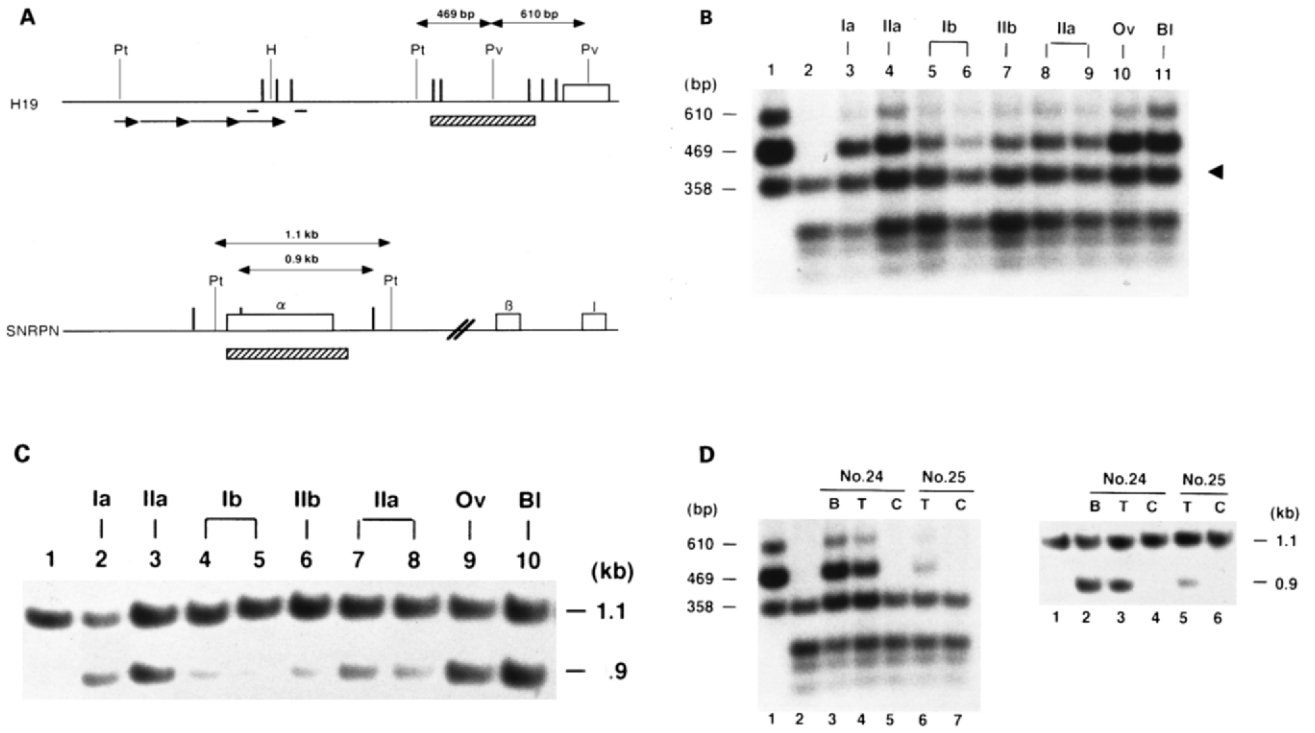

Figure 3 Methylation analyses of the *H19* and *SNRPN* genes in teratomas. *A,* Schematic restriction maps of analyzed regions. Exons are depicted by unblackened boxes. Probes are indicated by hatched boxes below the lines. Arrows represent the CpG-rich repeated sequences. Only the analyzed *Hpa*II (*H19*) and *Not*I (*SNRPN*) sites are shown, indicated by vertical thick lines. The polymorphic *Hha*I (H) site is indicated, along with primers that were used in the PCR-based methylation analysis. Restriction sites are as follows: Pt = *Pst*I and Pv = *Pvu*II. *B,* Southern-blot analysis of *H19* methylation. *Pst*I and *Pvu*II-cleaved DNA were subjected to *Hpa*II digestion (lanes 3–11) or *Msp*I digestion (lane 2). Digestion with *Pst*I/*Pvu*II alone is shown in lane 1. An arrowhead indicates the internal control used to calibrate the loaded amounts of DNA. The 469-bp *Pst*I-*Pvu*II fragment was quantified. The groups to which the teratomas belong are indicated at the top. "Ov" denotes normal portion of the ovary from a patient who had a teratoma and "Bl" denotes peripheral blood DNA. *C,* Southern-blot analysis of *SNRPN* methylation. DNA samples were digested with *Pst*I alone (lane 1) or *Pst*I plus *Not*I (lanes 2–10). *D,* Changes in methylation states in the *H19* (*left panel*) and *SNRPN* (*right panel*) genes, after cultivation. In two cases of teratomas, DNA samples were obtained from cultured cells (C) or directly from the tumor tissues (T). B = host-blood DNA.

57°C, and extension for 30 s at 72°C with primers A and B, with 0.5 μg genomic DNA as template; nested PCR, 15 cycles at 94°C for 30 s, 57°C for 30 s, and 72°C for 30 s with primers a and b, with 2 μl of 10-fold diluted first PCR product as template. Primers were as follows: primer A, 5′-TACCTCCCAGCCACTTCC; primer B, 5′-TGCACTGCGGCAAACAAGCA; primer a, 5′-CACTGTCACACCGACTCATC; and primer b, 5′-TGCCTGACGCATCTGTCTGA.

Allelic Analysis of Methylation

Using the *Hha*I polymorphism, we examined the allele specificity of methylation for the candidate region of the human *H19* locus, which has previously been shown to display a paternal-specific methylation imprint (Jinno et al. 1996). In brief, genomic DNA with or without prior digestion with a methyl-sensitive enzyme *Hpa*II was PCR amplified. The product was restricted with *Hha*I and separated onto a 4% polyacrylamide gel. The allele specificity of methylation of the *Not*I sites of *SNRPN,* described above, was similarly examined with a PCR-based assay with use of the *Hpa*II/*Msp*I polymorphism in the first intron of the *SNRPN* gene (Saitoh et al. 1997).

Results

Genotype Analysis

The genotype in each of 25 benign ovarian teratomas was compared with that of a peripheral blood sample

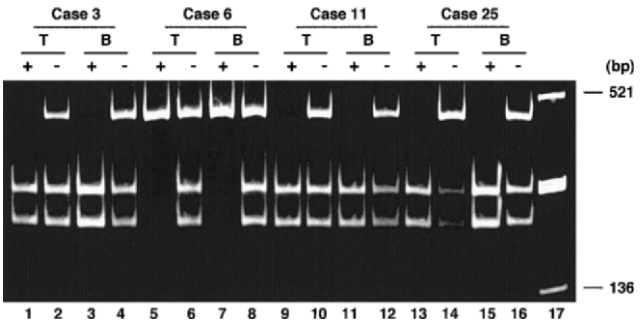

Figure 4 PCR-based methylation assay of *H19*. Allele specificity of *H19* methylation in teratomas was examined with the *Hha*I RFLP. DNA pretreated with *Hpa*II (+) or without *Hpa*II (−) was PCR amplified, *Hha*I digested, and separated onto a 4% polyacrylamide gel. T = tumor DNA; B = host-blood DNA.

from their respective hosts. CA-repeat markers were exclusively used in the present study because of their abundance and availability. PCR amplification of dinucleotide repeats yields slippage products that occasionally render the electrophoretic patterns of the product difficult to read. However, tetranucleotide repeats, which give less-ambiguous data, confirmed the preliminary results of genotyping with CA-repeat markers.

None of the markers that were heterozygous in the host's peripheral blood showed complete homozygosity in the matched teratoma. Instead, there were differences in relative intensity between the two alleles in the teratoma when compared with that of the corresponding alleles of the host (fig. 2). Such alterations seem to be best explained by the presence of at least two cell populations with different genotypes in the single tumor. This interpretation was supported by the observation that DNA prepared from cultured cells of two teratomas revealed complete homozygosity at all loci, whereas DNA directly extracted from the tumors showed only a shift in relative allele intensity (data not shown). In the present study, we regarded a consistent difference in allele intensity between the tumor and host for multiple markers to be evidence of homozygosity, regardless of the degree of such differences.

The genotype data were used to infer the origins of these teratomas. Pericentromeric markers were first used to classify the teratomas into two groups: teratomas showing a heterozygous (group I) or a homozygous (group II) pattern in all or almost all of the markers. Each group was then subdivided into teratomas showing evidence of recombination at multiple loci on two or more chromosomes (subgroups Ib and IIb) or showing no evidence of recombination (subgroups Ia and IIa) (table 1). Thus, the origin of each subgroup of teratomas can be inferred, as given in figure 1. Teratomas in group Ia may have originated from premeiotically dividing germ cells as well as from immature primary oocytes; a somatic-cell origin could not be completely excluded despite the methylation patterns for two imprinted genes as described in "Methylation Analysis," below. Group IIa includes teratomas that might have arisen from apparently immature primary oocytes—perhaps totally devoid of recombination between homologous chromosomes—that may have initiated premature meiotic division followed by subsequent mitotic division and cell proliferation. Teratomas in group Ib possibly were generated from primary oocytes that had proceeded to undergo meiotic recombination. The group IIb teratomas should have arisen by meiosis II error after completion of meiosis I. Of the 25 teratomas studied, seven (28%) belonged to group Ia, six (24%) to group IIa, eight (32%) to group Ib, and one (4%) to group

Table 2

Relative Intensities of *Hpa*II- or *Not*I-Resistant Bands of the *H19* or *SNRPN* Gene in Teratomas, Compared with Those in the Host's Blood DNA

Group and Case[a]	Relative Intensity of[b] *H19*	*SNRPN*
Ia:		
4	.84	1.05
6	.91	.98
15	1.17	NA
16	1.12	1.02
19	.78	1.04
Mean ± SD	.96 ± .15	1.02 ± .03
IIa:		
1	.84	1.16
3	.48	1.36
10	.48	1.35
17	.72	1.17
22	.54	1.34
23	.65	1.13
Mean ± SD	.62 ± .13	1.25 ± .10
Ib:		
5	.53	1.29
12	.40	1.62
13	.46	1.33
18	.31	1.57
24	.59	1.21
24C	.00	1.82
25	.21	1.66
25C	.03	2.07
Mean ± SD	.42 ± .13	1.45 ± .18
IIb:		
11	.36	1.65
Not determined:		
20	.72	1.25
21	.63	1.26

[a] A "C" suffix denotes cultured cells and a case that therefore was excluded from calculation of the mean value.

[b] As determined, in most cases, in two to four experiments. NA = not analyzed.

IIb. Three teratomas were "unclassified" under the above grouping criteria (table 1). Thus, among 25 teratomas, there was only one case whose origin could be attributed to a failure of meiosis II disjunction. This incidence is very low compared with previous reports.

Methylation Analysis

Two oppositely imprinted human genes were chosen for methylation analysis: the paternally imprinted *H19* and maternally imprinted *SNRPN*. CpG islands with possible methylation imprints have been identified in the 5′ upstream region of *H19* and in the exon α and its flanking regions of *SNRPN* (Sutcliffe et al. 1994; Buiting et al. 1995; Jinno et al. 1996; Kubota et al. 1996). *Hpa*II sites present in this region of *H19* are heavily methylated in sperm and are methylated only on the paternal allele in somatic cells, whereas *Not*I sites of *SNRPN* are methylated only on the maternal allele in various tissues.

The methylation status of the *Hpa*II and *Not*I sites in those regions of *H19* and *SNRPN,* respectively, were examined by Southern blot hybridization (fig. 3) and PCR-based assay of the teratomas (fig. 4). Unexpectedly, *H19* was partially methylated to various degrees in all teratomas examined (fig. 3*B*). The 469-bp *Hpa*II-resistant (i.e., methylated) bands took values in intensity with a range of 0.21–1.17, compared with those of the host's peripheral blood DNA. The mean ± SD values of each group were 0.96 ± 0.15 ($n = 5$) for Ia, 0.62 ± 0.13 ($n = 6$) for IIa, and 0.42 ± 0.13 ($n = 6$) for Ib, which suggests that the degree of methylation progressively decreased as the presumptive origin of the tumors advanced through the stages of oogenesis. *SNRPN* was also partially methylated but tended to be more heavily methylated than in the host's blood DNA (fig. 3*C*). The relative intensities of *Not*I-resistant bands to net intensities (*Not*I-resistant bands plus *Not*I-cleaved bands) had a range of 0.98–1.66, compared with those of the host's blood DNA. The mean values of each group of teratomas were 1.02 ± 0.03 ($n = 4$) for Ia, 1.25 ± 0.10 $n = 6$) for IIa, and 1.45 ± 0.18 $n = 6$) for Ib, which suggests that, unlike *H19,* the methylation of *SNRPN* progressively increased as the stage of germ cells from which the tumors were presumed to have arisen increased (table 2). Consistent with these average findings, there was a clear reciprocal correlation between methylation levels of *H19* and *SNRPN* when data for individual teratomas were plotted (fig. 5). DNA prepared from cultured cells of two teratomas was found to be extremely undermethylated in *H19* and hypermethylated in *SNRPN,* whereas the original tumor tissues showed partial methylation for both genes (fig. 3*D*).

The allele specificity of partial methylation was examined with the PCR-based methylation assay. Either of the *H19* alleles was amplified after *Hpa*II digestion of teratoma DNA, and this was the same allele that showed resistance to *Hpa*II digestion in the host's blood DNA (fig. 4). Analyses of *SNRPN* gave similar results; again, the methylated allele in the host's blood DNA was predominantly or exclusively amplified in the teratoma after *Not*I digestion (data not shown).

Discussion

The germ-cell origin of benign ovarian teratomas is well established, by features such as homozygosity for genetic polymorphisms that are heterozygous in the hosts and crossover events. Our comprehensive genotype analysis of these tumors, using microsatellite-repeat polymorphisms, suggested the presence of heterogeneous cell populations with different genotypes within individual tumors. Furthermore, DNA prepared from cultured cells of two teratomas showed homozygosity for markers and extreme undermethylation of *H19* and extreme hypermethylation of *SNRPN,* whereas the original tumors were partially methylated in both of the genes. Although it is evident that selection occurred in cells with different genotypes during cell culture, it is unclear whether differences in epigenotype were causatively involved in the growth selection of cells in the tumors. It is unlikely that this genetic and epigenetic heterogeneity results from normal tissue contamination, because (*a*) the tumors were well isolated from normal tissues, by the capsule, and (*b*) DNA obtained from different portions of tumors gave similar results. Rather, this finding seems to provide additional evidence supporting the germ-cell origin of benign ovarian teratomas (fig. 1).

The present study revealed a low incidence (4%) of teratomas originating from secondary oocytes, a finding that seems reasonable when the relatively short duration of the meiosis II phase during oogenesis is considered. Discrepancies between the current and previous studies may arise from differences in the methods used to detect homozygosity (Linder et al. 1975; Dahl et al. 1990; Deka et al. 1990). First, the choice of polymorphic marker varied among these studies. Chromosome polymorphisms would not distinguish group IIa (MI error) from group IIb (MII error) teratomas, and RFLP analysis of DNA polymorphisms gives more-limited information than microsatellite analyses. Second, the results obtained by direct analysis of teratoma tissue may differ from those obtained with cultured cells. In the present study, cultured cells exhibited homogeneity in both genotypes

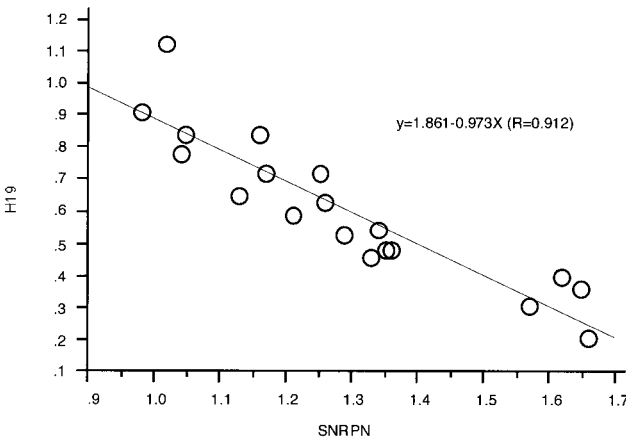

Figure 5 Correlation of the *H19* and *SNRPN* methylations in teratomas. In comparison to the blood DNA, relative intensities of the *Hpa*II-resistant band of *H19* as shown in figure 3 were plotted against those of the *Not*I-resistant band of *SNRPN*.

and epigenotypes, whereas the original tumor tissues showed heterogeneity. Although only two teratomas and two imprinted genes were analyzed in this way, the cultured cells closely matched the expected features of the female gamete. This finding may be relevant, given that cytogenetic studies are usually performed in cultured cells. The molecular basis of chromosome-painting polymorphisms/heteromorphisms is unclear, and it is possible that they are affected by the process of imprinting. Finally, a third possibility is that differences in environmental as well as genetic factors may influence the incidence with which teratomas arise from each stage of oogenesis (Eppig et al. 1996).

H19 is a typical example of a paternally imprinted gene. The gene is heavily methylated in sperm, and only the paternal allele is methylated in somatic cells. Thus, hypomethylation of *H19* was expected in the benign ovarian teratomas, because they are derived from female germ cells. However, teratomas showed various degrees of methylation ranging from hypomethylation to the level that is normal for somatic cells. The allele with residual methylation was always the same as that in the host's peripheral blood and was therefore of paternal origin. These findings suggest that the primary imprint of *H19* is not completely erased until late oogenesis. On the other hand, *SNRPN* is a maternally imprinted gene, with the maternal allele being methylated in somatic cells, and it was expected to show hypomethylation or hypermethylation in teratomas depending on the stage in oogenesis from which each tumor arose. As with *H19* methylation, *SNRPN* showed partial methylation, to various degrees, from normal somatic-cell level to hypermethylation. This observation suggests that the methylation imprint of *SNRPN* may not be fully established until an advanced stage of female gametogenesis. It has been suggested that epigenetic modification of the *Igf2r* gene occurred late in oogenesis in mice, by use of nuclear transfer techniques (Kono et al. 1996). In a related experiment, the *Snrpn* gene was shown to be expressed from the nongrowing oocytes-derived alleles in experimental parthenogenetic embryos, whereas expression of *Snrpn* from the fully grown oocytes-derived alleles was suppressed. By contrast, *H19* was expressed equivalently by both the nongrowing and fully grown oocytes-derived alleles, indicating that *H19* imprinting is established early in mice (Obata et al. 1998). This apparent difference in timing of *H19* imprinting between humans and mice may result from the sequence divergence in the corresponding regions proposed to be the site of primary methylation imprints (Tremblay et al. 1995; Jinno et al. 1996). Another explanation is that the regions analyzed in methylation states, in the present study, do not strictly represent the methylation imprints, unlike those identified in mouse *H19* and *Igf2r* (Stöger et al. 1993; Tremblay et al. 1995; Wutz et al. 1997; Thorvaldsen et al. 1998). In this case, they may just be indicators. In either case, they can be considered to reflect the state of the primary imprints.

It remains to be ascertained whether the methylation imprints analyzed here have any bearing on regulated imprinted expression of the genes studied. In a preliminary experiment, allelic-expression analysis was performed in a limited number of available and informative RNA samples (data not shown). Biallelic expression of *H19,* with varying degrees of difference in intensity between the alleles, was shown in three group Ia teratomas and in one group IIb teratoma. This finding is consistent with the expectation of full expression from the maternal allele and partial or variable expression from the other allele. By contrast, monoallelic expression of *SNRPN* was observed in two group Ia teratomas (data not shown). Again, this finding is consistent with the expectation of methylation of the (maternal) allele and expression from the other allele, which is methylated in some cell populations and unmethylated in other populations.

When the teratomas were grouped according to their assumed origin-in-stage at oogenesis, the mean intensity of the *Hpa*II-resistant band for *H19* gradually decreased as the stage of oogenesis advanced. By contrast, the mean intensity of the *Not*I-resistant band for *SNRPN* progressively increased with advancing stage of oogenesis. Similarly, a clear correlation was obtained between *H19* undermethylation and *SNRPN* heavy methylation, as exhibited in a regression line with regression ratio of 0.912, when their methylation levels in individual teratomas were plotted. Although interpretation of the above data is complicated by the fact that the teratoma consists of heterogeneous cell populations, it appears

that even cells with the same genotype had different methylation states in *H19* and *SNRPN*. It is tempting to speculate on the presence of some mechanistic links in the primary imprinting process directed to the opposite aims, that is, activating and protecting from methylation. Methylation analyses must be extended to more imprinted genes to see the relevance of this speculation.

In humans, studies in female germ cells are ethically very limited. With the assumption that methylation imprints are neither erased in somatic cells during cleavage nor added during somatic development, we have used benign ovarian teratomas to study the interrelationship of the methylation states of the imprinted genes *H19* and *SNRPN* during the gametic-imprinting process in ova. The presence of heterogeneous cell populations in teratomas may complicate the interpretation of methylation or expression data on imprinted genes. If the relationship between the degree of methylation and grouping of the teratomas seen here can be applied to other imprinted genes, and if all cultured cells show purity of genetic and epigenetic nature, as found in our two cases, then teratomas could be a useful tool for such studies. That subset of teratomas in which the imprinting pattern is well established and is as expected for maternal chromosomes may be particularly valuable in this regard.

Although inferences can be drawn, the precise methylation states of the imprinted genes in the germ cells from which the tumors originated is not known, and our study may instead provide insights into somatic events in methylation imprinting during tumorigenesis. For example, such data could be interpreted to indicate that methylation imprints in the *H19* or *SNRPN* gene are erased or established in somatic cells during tumor development. Evidence supporting the erasure of methylation and de novo methylation in somatic cells is provided by the de novo methylation of *H19* in primary embryonic fibroblasts rescued from chimeras of female embryonic germ cells (Tada et al. 1998). In addition, reprogramming of the human *H19* methylation imprint has been observed in mouse-embryonic carcinoma cell lines containing a human chromosome 11, introduced by microcell-mediated chromosome transfer (Mitsuya et al. 1998). We consider that, collectively, these studies suggest that primary gametic imprinting may be a progressive and cumulative process that develops throughout gametogenesis. Incomplete organization of the imprint in *H19* may permit de novo methylation in some somatic cells during tumorigenesis, but, because of its heritability, formation of the complete imprint may eventually be achieved, and thereafter the incidentally acquired methylation may no longer be sustained. A similar scenario may be drawn for the imprinting of *SNRPN*, but in the opposite direction with respect to methylation.

Acknowledgments

We appreciate Dr. Marion Maw's comments during manuscript preparation and Dr. Hisayoshi Nakajima's technical advice. The present study was supported by a Grant-in-Aid for Scientific Research from the Ministry of Education, Science and Culture of Japan and by Research on Human Genome and Gene Therapy from the Ministry of Health and Welfare of Japan.

Appendix

Microsatellite DNA Markers Used for Genotype Analysis of 25 Benign Ovarian Teratomas

In the following list, the tetranucleotide-repeat markers are underlined.

Pericentromeric Markers (16 Chromosomes, 25 Loci)	Noncentromeric Markers (3 Chromosomes, 20 Loci)
D2S113 (cen)	D6S1574
D4S2974 (4p12-q12)	D6S426
D5S2087 (cen)	D6S407 (6q16.3-q23.2)
D6S1573 (6p21-p12)	D6S314 (6q16.3-q27
D6S1681 (6q13)	D6S1654 (6q25)
D7S691 (7p13-cen)	D6S1719 (6q25.2-27
D7S2422 (cen)	D6S1590 (6q25.2-27)
D9S1799	D6S281 (6q27)
D11S905 (11p12)	D11S922 (11p15.5)
D11S1344 (11p11)	D11S1760 (11p15)
D11S4113 (11q13)	D11S1349 (11p15.4)
D14S990 (14q11.2)	D11S4190 (11p15)
D15S986 (15q12)	D11S4152 (11p14)
D15S1002 (15q13-q14)	D11S4200 (11q14-p13)
D16S3080 (16q12.1)	D11S4176 (11q14)
D18S453 (18p11.2-p11.1)	D11S4085 (11q25)
D19S410 (19p13.1)	D15S978 (15q15-q21)
D20S884 (20p11-q11.2)	D15S988 (15q22-tel)
D21S1899 (21q21)	D15S1014 (15q22-tel)
D22S1158 (22p11.2)	D15S966 (15q26-tel)
DXS991 (Xp11.21)	
D4S1645	
D7S1830	
D9S1124	
D11S2365	

Electronic-Database Information

Accession numbers and URLs for data in this article are as follows:

Cooperative Human Linkage Center, http://lpg.nci.nih.gov/CHLC/ (for microsatellite markers)

GenBank, http://www.ncbi.nlm.nih.gov/Web/Genbank/index.html (for DNA probe nested primers [U41384])
Généthon, http://www.genethon.fr (for microsatellite markers)
Online Mendelian Inheritance in Man (OMIM), http://www.ncbi.nlm.gov/Omim (for benign ovarian teratomas [MIM 166950] and complete hydatidiform moles [MIM 231090])

References

Buiting K, Saitoh S, Gross S, Dittrich B, Schwartz S, Nicholls RD, Horsthemke B (1995) Inherited microdeletions in the Angelman and Prader-Willi syndromes define an imprinting centre on human chromosome 15. Nat Genet 9:395–400

Dahl N, Gustavson KH, Rune C, Gustavsson I, Pettersson U (1990) Benign ovarian teratomas: an analysis of their cellular origin. Cancer Genet Cytogenet 46:115–123

Deka R, Chakravarti A, Surti U, Hauselman E, Reefer J, Majumder PP, Ferrell RE (1990) Genetics and biology of human ovarian teratomas. II. molecular analysis of origin of nondisjunction and gene-centromere mapping of chromosome 1 markers. Am J Hum Genet 47:644–655

Dib C, Faure S, Fizames C, Samson D, Drouot N, Vignal A, Millasseau P, et al (1996) A comprehensive genetic map of the human genome based on 5,264 microsatellites. Nature 380:152–154

Eppig JJ, Wigglesworth K, Varnum DS, Nadeau JH (1996) Genetic regulation of traits essential for spontaneous ovarian teratocarcinogenesis in strain lt/sv mice: aberrant meiotic cell cycle, oocyte activation, and parthenogenetic development. Cancer Res 56:5047–5054

Jinno Y, Yun K, Nishiwaki K, Kubota T, Ogawa O, Reeve AE, Niikawa N (1994) Mosaic and polymorphic imprinting of the WT1 gene in humans. Nat Genet 6:305–309

Jinno Y, Sengoku K, Nakao M, Tamate K, Miyamoto T, Matsuzaka T, Sutcliffe JS, et al (1996) Mouse/human sequence divergence in a region with a paternal-specific methylation imprint at the human H19 locus. Hum Mol Genet 5: 1155–1161

Kono T, Obata Y, Yoshimzu T, Nakahara T, Carroll J (1996) Epigenetic modifications during oocyte growth correlates with extended parthenogenetic development in the mouse. Nat Genet 13:91–94

Kubota T, Aradhya S, Macha M, Smith AC, Surh LC, Satish J, Verp MS, et al (1996) Analysis of parent of origin specific DNA methylation at SNRPN and PW71 in tissues: implication for prenatal diagnosis. J Med Genet 33:1011–1014

Li E, Beard C, Jaenisch R (1993) Role for DNA methylation in genomic imprinting. Nature 366:362–365

Linder D, McCaw BK, Hecht F (1975) Parthenogenic origin of benign ovarian teratomas. N Engl J Med 292:63–66

Mansfield DC, Brown AF, Green DK, Carothers AD, Morris SW, Evans HJ, Wright AF (1994) Automation of genetic linkage analysis using fluorescent microsatellite markers. Genomics 24:225–233

Mitsuya K, Meguro M, Sui H, Schulz TC, Kugoh H, Hamada H, Oshimura M (1998) Epigenetic reprogramming of the human H19 gene in mouse embryonic cells does not erase the primary parental imprint. Genes Cells 3:245–255

Murray JC, Buetow KH, Weber JL, Ludwigsen S, Scherpbier-Heddema T, Manion F, Quillen J, et al (1994) A comprehensive human linkage map with centimorgan density: Cooperative Human Linkage Center (CHLC). Science 265: 2049–2054

Obata Y, Kaneko-Ishino T, Koide T, Takai Y, Ueda T, Domeki I, Shiroishi T, et al (1998) Disruption of primary imprinting during oocyte growth leads to the modified expression of imprinted genes during embryogenesis. Development 125: 1553–1560

Razin A, Cedar H (1994) DNA methylation and genomic imprinting. Cell 77:473–476

Saitoh S, Buiting K, Cassidy SB, Conroy JM, Driscoll DJ, Gabriel JM, Gillessen-Kaesbach G, et al (1997) Clinical spectrum and molecular diagnosis of Angelman and Prader-Willi syndrome patients with an imprinting mutation. Am J Med Genet 68:195–206

Stöger R, Kubicka P, Liu CG, Kafri T, Razin A, Cedar H, Barlow DP (1993) Maternal-specific methylation of the imprinted mouse igf2r locus identifies the expressed locus as carrying the imprinting signal. Cell 73:61–71

Surti U, Hoffner L, Chakravarti A, Ferrell RE (1990) Genetics and biology of human ovarian teratomas. I. Cytogenetic analysis and mechanism of origin. Am J Hum Genet 47: 635–643

Sutcliffe JS, Nakao M, Christian S, Örstavik KH, Tommerup N, Ledbetter DH, Beaudet AL (1994) Deletions of a differentially methylated CpG island at the SNRPN gene define a putative imprinting control region. Nat Genet 8:52–58

Tada T, Tada M, Hilton K, Barton SC, Sado T, Takagi N, Surani MA (1998) Epigenotype switching of imprintable loci in embryonic germ cells. Dev Genes Evol 207:551–561

Thorvaldsen JL, Duran KL, Bartolomei MS (1998) Deletion of the H19 differentially methylated domain results in loss of imprinted expression of H19 and Igf2. Genes Dev 12: 3693–3702

Tremblay KD, Saam JR, Ingram RS, Tilghman SM, Bartolomei MS (1995) A paternal-specific methylation imprint marks the alleles of the mouse H19 gene. Nat Genet 9:407–413

Wutz A, Smrzka OW, Schweifer N, Schellander K, Wagner EF, Barlow DP (1997) Imprinted expression of the Igf2r gene depends on an intronic CpG island. Nature 389:745–749